Number of discernible object colors is a conundrum

Kenichiro Masaoka,[1,2,*] Roy S. Berns,[2] Mark D. Fairchild,[2] and Farhad Moghareh Abed[2]

[1]*NHK Science & Technology Research Laboratories, Tokyo 157-8510, Japan*
[2]*Munsell Color Science Laboratory, Chester F. Carlson Center for Imaging Science, Rochester Institute of Technology, Rochester, New York 14623, USA*
**Corresponding author: masaoka.k-gm@nhk.or.jp*

Received June 15, 2012; revised December 19, 2012; accepted December 24, 2012; posted January 2, 2013 (Doc. ID 169396); published January 31, 2013

Widely varying estimates of the number of discernible object colors have been made by using various methods over the past 100 years. To clarify the source of the discrepancies in the previous, inconsistent estimates, the number of discernible object colors is estimated over a wide range of color temperatures and illuminance levels using several chromatic adaptation models, color spaces, and color difference limens. Efficient and accurate models are used to compute optimal-color solids and count the number of discernible colors. A comprehensive simulation reveals limitations in the ability of current color appearance models to estimate the number of discernible colors even if the color solid is smaller than the optimal-color solid. The estimates depend on the color appearance model, color space, and color difference limen used. The fundamental problem lies in the von Kries-type chromatic adaptation transforms, which have an unknown effect on the ranking of the number of discernible colors at different color temperatures.

OCIS codes: 330.1730, 330.4060, 330.5020, 120.5240, 230.6080, 300.6170.

1. INTRODUCTION

The number of discernible object colors is informative not only because of scientific interest in human color vision but also because of its potential use in industrial applications such as the development of pigments and dyes, evaluation of the gamut coverage of displays, and design of the spectral power distribution of light sources. The color gamut of color imaging media and its main controlling factor, the viewing conditions, are of significant practical as well as theoretical importance in the reproduction of color images [1]. However, widely varying estimates of the number of discernible colors have been made over the past 100 years. This motivated us to clarify the source of the variation and derive a more accurate estimate.

Perceptible color is represented in a color solid on the basis of the trichromatic nature of human vision, where a color solid is a three-dimensional representation of a color model. Perceptual color space can be reasonably represented in cylindrical coordinates (hue, chroma/colorfulness, and lightness/brightness) or Cartesian coordinates (two opponent-color dimensions and lightness/brightness). The number of discernible colors contained in a three-dimensional solid in a perceptual color space has been estimated using different methods. Kuehni [2] has summarized the early research. Unfortunately, some of these studies do not provide sufficient detail. To make matters worse, some estimates by authorities have been used repeatedly in other journal papers and books without reference to the original estimates, which makes it difficult to identify the authorities. Here, we investigate the original estimates in detail, referring to Kuehni's summary, and add some recent estimates, as summarized in Table 1.

In 1896, Titchener [3] experimentally identified 30,850 visual sensations (700 "brightness qualities" + 150 "spectral colors" + 30,000 "color sensations of mixed origin"). Later, he modified his estimate to 32,820 visual sensations (660 + 160 + 32,000) in his revised book [4]. In 1939, Boring *et al.* [5] explained that there are 156 just-noticeable differences (JNDs) in hue, 16–23 JNDs in saturation, and 572 JNDs in brightness, but he somehow made an inflated estimate of the number of discriminably different colors, on the order of 300,000, which is comparable to his estimate of the number of discernible tones that differ either in pitch or in loudness. He said, "In a sense there are, speaking generally, about as many tones as colors." Also in 1939, Judd and Kelly [6] estimated that about 10 million colors are distinguishable in daylight by the trained human eye, although they did not mention the grounds for their estimate and other details (e.g., criteria for color differences, assumed illuminant). This figure of 10 million was also used in the book by Judd and Wyszecki [7]. In 1951, Halsey and Chapanis [8] stated that a normal observer can discriminate well more than 1 million different colors under ideal, laboratory conditions of observation. However, in 1981, Hård and Sivik [9] stated that our ability to identify a given color with some certainty is a great deal less and would probably cover only about 10,000–20,000 colors.

In addition to these results, recent estimations were made using optimal colors (i.e., optimal-color solids). An optimal color is the nonfluorescent object color having the maximum saturation under a given light. Ostwald [10] empirically found that optimal-color reflectances are either 0 or 1 at all wavelengths with at most two transitions. The first mathematical proof of this, which uses the convexity of the spectrum locus, is attributed to Schrödinger [11]. Following the calculation of optimal colors by Luther [12], Nyberg [13], and Rösch [14], MacAdam generated a geometric proof of the optimal-color theorem using the CIE xy chromaticity diagram [15] and calculated the chromaticity coordinates of the optimal-color loci,

Table 1. History of the Estimates of the Number of Discernible Colors

Year	Researcher	Estimate	Illuminant	Color Data/Color Model
1896	Titchener [3]	30,850		700 "brightness qualities" + 150 "spectral colors" + 30,000 "colors mixed with origin"
1899	Titchener [4]	32,820		660 "brightness qualities" + 160 "spectral colors" + 32,000 "colors mixed with origin"
1939	Boring *et al.* [5]	300,000		156 hue × 16–23 saturation × 572 brightness
1939	Judd and Kelly [6]	10,000,000		Unknown
1943	Nickerson and Newhall [17]	7,295,000		Optimal color solid/Munsell notation
1951	Halsey and Chapanis [8]	1,000,000		Unknown
1981	Hård and Sivik [9]	10,000–20,000		Unknown
1998	Pointer and Attridge [18]	2,280,000	D65	Optimal color solid/CIELAB
2007	Wen [19]	352,263	D65	Optimal color solid/CIE94
2007	Martínez-Verdú *et al.* [20]	2,050,000	E	Optimal color solid/CIECAM02 lightness–colorfulness (Ja_Mb_M)
		2,046,000	C	
		2,013,000	D65	
		1,968,000	F7	
		1,753,000	A	
		1,735,000	F11	
		1,665,000	F2	
2008	Morovic [22]	1,900,000	D50	Optimal color solid/CIECAM02 lightness–chroma (Ja_Cb_C)
2012	Morovic *et al.* [23]	4,200,000	F11	Optimal color solid/CIECAM02 lightness–chroma (Ja_Cb_C)
		3,800,000	D50	
		3,500,000	A	
		1,700,000	D50	LUTCHI/CIECAM02 lightness–chroma (Ja_Cb_C)

called the MacAdam limits, under illuminants A and C, with luminous reflectance Y for the third dimension [16].

In 1943, Nickerson and Newhall [17] applied the Munsell notation to the MacAdam limits and identified a total of 5836 full chroma steps for 40 hues spaced 2.5 hue steps apart, and nine values spaced one value step apart. They estimated the number of discriminable colors as 7,295,000, assuming that one chroma, hue, or value step corresponds to 5, 2, and 50 JNDs, respectively. In 1998, Pointer and Attridge [18] counted the unit cubes within an optimal-color solid under illuminant D65 in the CIE 1976 (L^*, a^*, b^*) color space (CIELAB) and made an estimate of about 2.28 million. In 2007, Wen [19] sliced an optimal-color solid under illuminant D65 at each lightness unit and divided each slice into pieces having the unit chroma and hue differences described in CIE94, obtaining a count of 352,263. Also in 2007, Martínez-Verdú *et al.* [20] counted unit cubes packed in optimal-color solids under several standard illuminants (A, C, D65, E, F2, F7, F11) and high-pressure sodium lamps in the lightness and colorfulness space (J, a_M, b_M) of the CIECAM02 color appearance model [21]. They assumed this to be the most uniform color space on the basis of their observation that the calculated optimal-color solids in the CIECAM02 color space were relatively spherical compared to those in the CIELAB color space and others. They estimated that there are 2.050 million distinguishable colors under illuminant E, 2.046 million under illuminant C, 2.013 million under illuminant D65, 1.968 million under illuminant F7, 1.753 million under illuminant A, and fewer colors under the other light sources. They also suggested the possibility of an alternative color-rendering index based on the number of discernible colors within an optimal-color solid. In 2008, Morovic [22] calculated the convex hull volume of optimal-color solids in the lightness and chroma space (J, a_C, b_C) of CIECAM02 and estimated a total of 1.9 million colors under illuminant D50. Using the same counting method and color space, in 2012, Morovic *et al.* [23] doubled the number to 3.8 million colors under illuminant D50, in addition to other estimates of 4.2 million under illuminant F11 and 3.5 million under illuminant A. On the other hand, Morovic *et al.* also pointed out that the currently available models failed to give predictions when extrapolating the psychophysical data they are based on; finally, they made an alternative, safe estimate of at least 1.7 million colors, which was their estimate of the color gamut volume of the LUTCHI [24] data used to build CIECAM02.

Unfortunately, it is unknown which estimate is the most reliable. The validity of even the estimates based on the color appearance models [18–20,22,23] has not been verified. To complicate matters, the recent estimates were made using different combinations of color appearance models (CIELAB and CIECAM02), color spaces (lightness–chroma and lightness–colorfulness), color difference limens (CIELAB unit, CIE94 color difference, and CIECAM02 unit), and lighting conditions (e.g., illuminants D50 and D65). It is important to clarify the source of the discrepancies in previous, inconsistent estimates and determine the limitations of the current color appearance models in both a theoretical and practical sense.

In this paper, we provide estimates of the number of discernible colors within the optimal-color solid for a wide range of color temperatures and illuminance levels, using a fast, accurate model for computing the optimal colors. Several chromatic adaptation models, color spaces, and color difference limens are used to verify the recent estimates based on color appearance models.

2. METHODS

Figure 1 shows a flowchart of the method used to compute an optimal color with a specified central wavelength under an illuminant having a given spectral power distribution and adaptation illuminance level. Optimal colors were searched

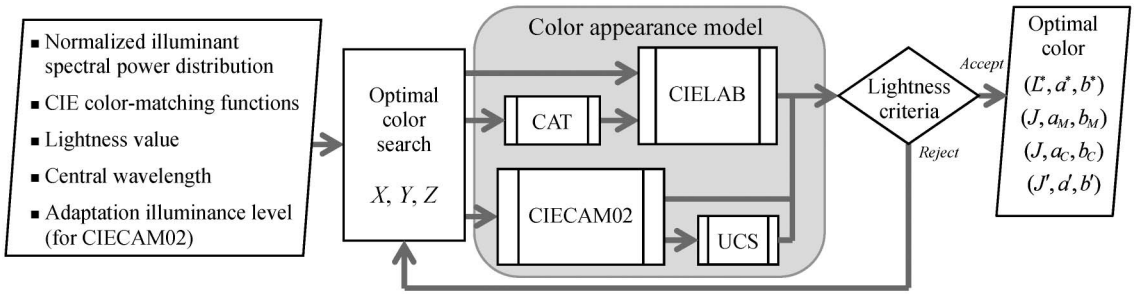

Fig. 1. Flowchart for computing an optimal color.

iteratively so that their lightness values were equalized to the given lightness values. To estimate the number of discernible colors within an optimal-color solid, we computed the optimal-color loci at regular lightness unit intervals of L^* in CIELAB, J in CIECAM02, and J' in a CIECAM02-based uniform color space (CAM02-UCS) [25]. Three different chromatic adaptation transformations (CATs) were embedded in front of CIELAB with a D65 reference white point. Blackbody radiators at color temperatures ranging from 2000 to 4000 K and standard daylight illuminants at CCTs ranging from 4000 to 10,000 K at 500 K intervals were used as light sources in the simulation. Illuminance levels of 200 lx (museum standard [26]), 1000 lx (reference viewing condition [27]), 10,000 lx (outside on cloudy days), and 100,000 lx (outside on sunny days) were considered for the reference white in CIECAM02. Additionally, illuminant E and illuminant series F (F1–F12) were used at an illuminance of 1571 lx to verify the results of Martínez-Verdú *et al.* [20].

A. Optimal-Color Computation

Optimal colors are generated using stimuli with either 0 reflectance (transmittance) at both ends of the visible spectrum and 1 in the middle (type I) or 1 at the ends and 0 in the middle (type II). Figure 2 illustrates both types, where $\lambda_{\text{cut-on}}$ and $\lambda_{\text{cut-off}}$ represent the cut-on and cut-off wavelengths, respectively. In our simulation, the end colors (high-pass and low-pass) are handled as type I, with the wavelength of transition ($\lambda_{\text{cut-on}}$ or $\lambda_{\text{cut-off}}$) being the end point of the visible spectrum.

A modified version of Masaoka's model [28] was used to calculate the tristimulus values of optimal colors. We used the CIE 1931 color-matching functions $\bar{x}$, $\bar{y}$, and $\bar{z}$ at wavelengths ranging from 400 to 700 nm at 1 nm intervals.

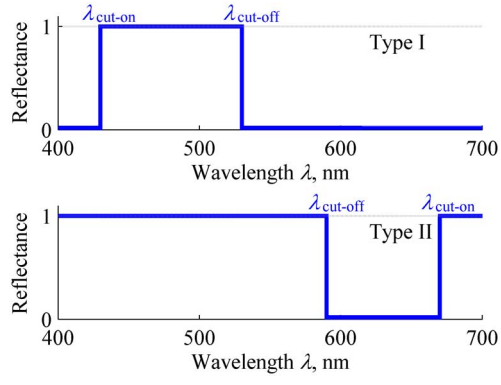

Fig. 2. (Color online) Two types of spectral reflectance (transmittance) for optimal colors.

The spectra of the daylight illuminants were calculated using the CIE equation [29]. Following the recommendation of CIE [30], spline interpolation was used for the CIE color-matching functions and daylight illuminant spectra in order to ensure a sufficiently small wavelength step of 0.1 nm. The blackbody radiation was calculated using Planck's law at wavelength intervals of 0.1 nm. The light source spectrum S was normalized so that $\Sigma_{k=1}^{N} S(k)\bar{y}(k) = 100$, where N is the number of wavelength steps, $N = 3001$.

To avoid switching between types I and II during optimization of $\lambda_{\text{cut-on}}$ and $\lambda_{\text{cut-off}}$, three copies of the color-matching functions $\bar{x}(k)$, $\bar{y}(k)$, and $\bar{z}(k)$, and illuminant spectrum $S(k)$ were each concatenated separately, forming four sequences denoted respectively as $\bar{x}_c$, $\bar{y}_c$, and $\bar{z}_c$, and S_c, as shown in the upper part of Fig. 3, where n is the central wavelength, and h_n is the half bandwidth of the spectral reflectance $R_n(l)$ of the optimal color on the concatenated wavelength scale l. Here, $l_{\text{cut-on}} = n - h_n$, and $l_{\text{cut-off}} = n + h_n$:

$$R_n(l) = \begin{cases} 1, & l_{\text{cut-on}} \le l \le l_{\text{cut-off}} \\ 0, & \text{otherwise} \end{cases}, \tag{1}$$

where n is an integer between $N+1$ and $2N$, and h_n is a real number between 0 and $N/2$. It is obvious that concatenation makes it possible to treat a type II band-stop reflectance as a

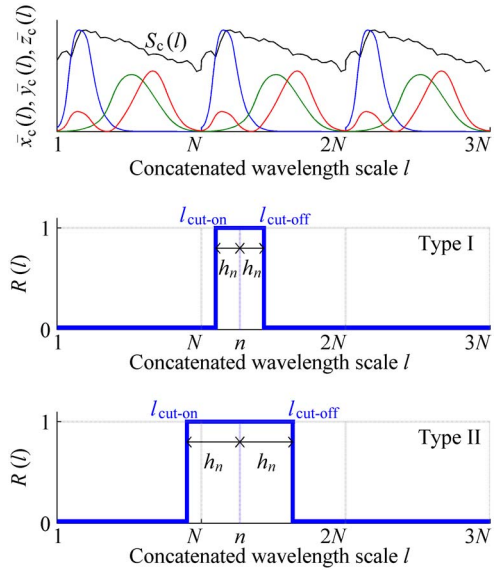

Fig. 3. (Color online) Concatenation of three copies of color-matching functions and illuminant spectrum (top). An optimal color has spectral reflectance $R(l)$ with central wavelength n and half bandwidth h_n on the concatenated wavelength scale l (center and bottom).

type I band-pass reflectance. Let $T_x(l)$, $T_y(l)$, and $T_z(l)$ be continuous functions obtained by linear interpolation of $S_c\bar{x}_c$, $S_c\bar{y}_c$, and $S_c\bar{z}_c$, respectively. Figure 4 shows a diagram illustrating trapezoidal integration of $T(l)$. The tristimulus values of the optimal color can be efficiently calculated using trapezoidal integration:

$$\begin{aligned} X_n &= \int R(l)T_x(l)\mathrm{d}l = \int_{l_{\text{cut-on}}}^{l_{\text{cut-off}}} T_x(l)\mathrm{d}l \\ &= (T_x(n-\lfloor h_n\rfloor-1)\cdot\{h_n\} + T_x(n-\lfloor h_n\rfloor) \\ &\quad\cdot(2-\{h_n\}))\cdot\{h_n\}/2 \\ &\quad + (T_x(n+\lfloor h_n\rfloor+1)\cdot\{h_n\} + T_x(n+\lfloor h_n\rfloor) \\ &\quad\cdot(2-\{h_n\}))\cdot\{h_n\}/2 \\ &\quad + \sum_{k=n-\lfloor h_n\rfloor}^{n+\lfloor h_n\rfloor} T_x(k) - T_x(n-\lfloor h_n\rfloor)/2 - T_x(n+\lfloor h_n\rfloor)/2. \quad (2) \end{aligned}$$

Here $\lfloor h_n\rfloor$ is the floor of h_n, and $\{h_n\}$ is the fractional part of h_n. The first two terms in Eq. (2) represent the end margins of the integral, and the other terms represent trapezoidal integration from $n-\lfloor h_n\rfloor$ to $n+\lfloor h_n\rfloor$. Y_n and Z_n are described by replacing T_x in Eq. (2) with T_y and T_z, respectively. The estimated tristimulus values of an optimal color were converted to the lightness value L_n by using a specified color appearance model. Here, h_n was optimized by a simplex method so that L_n becomes equal to a specified lightness value L_{const} with an accuracy of $\pm10^{-7}$. The termination tolerance for h_n was set to 10^{-10} on the concatenated wavelength scale or 10^{-11} nm. The MATLAB code we used is presented in the appendix. The MATLAB *fminsearch* function was used to search for a local minimizer h_n of the function $|L_{\text{const}}-L_n|$ in a specified range from 0 to $N/2$.

This method is more computationally efficient and accurate than other methods. In the method of Martínez-Verdú *et al.* [20], the algorithm computes optimal colors with all the possible pairs of $\lambda_{\text{cut-on}}$ and $\lambda_{\text{cut-off}}$ at 0.1 nm wavelength intervals and looks for the optimal colors whose lightness values are equal to a given lightness with a given tolerance. They suggested 0.01 for the lightness tolerance in order to obtain adequate samples of optimal colors to form a locus. However, the lightness tolerance obtained using such a trial-and-error method is not always appropriate for an arbitrary illuminant. Another problem is the computational cost. It took about 1 h for each optimal-color type and lightness. In the method of Li *et al.* [31], the algorithm finds reflectance values at intervals of 1 nm instead of 0.1 nm. The computational cost is less than that of Martínez-Verdú *et al.*'s method; it took several minutes to obtain a locus. The discrete reflectance values are either 1 or 0 at all wavelengths except for $\lambda_{\text{cut-on}}$ or $\lambda_{\text{cut-off}}$, where a value between 0 and 1 can be set, which enables the resulting loci to be smoother than those obtained by Martínez-Verdú *et al.*'s method, despite the sparse wavelength intervals. The spectral reflectance including a non-zero and non-one value is, however, no longer that of the optimal color by definition. The tolerances of the optimized parameters are unknown. The 1 nm wavelength intervals degrade the accuracy of optimal-color computation under spiky-spectrum illuminants. On the other hand, our method optimizes $\lambda_{\text{cut-on}}$ and $\lambda_{\text{cut-off}}$ for an optimal color on a continuous scale rather than finding discrete reflectance values. Prevention of switching between type I and type II dramatically reduced the computational cost; it took only about 10 s to obtain each locus. This computational efficiency enabled us to compare the estimates over a wide range of color temperatures and illuminance levels using several color models.

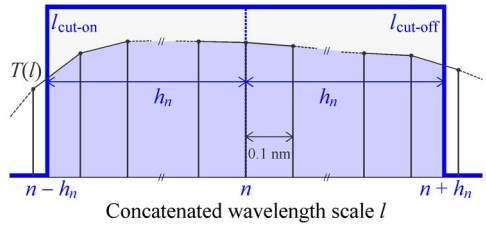

Fig. 4. (Color online) Diagram of trapezoidal integration of $T(l)$.

B. Color Appearance Model

We used CIELAB with three different CATs to verify the estimates of Pointer and Attridge [18]. In CIELAB, the vertical dimension represents the lightness L^*, which ranges from 0 to 100; the two horizontal dimensions represent the opponent red/green channel a^* and yellow/blue channel b^*. The CIELAB color space can also be represented in cylindrical coordinates using the chroma C^*_{ab} and hue h_{ab}. A model that contains predictors of at least the relative color appearance attributes of lightness, chroma, and hue is referred to as a color appearance model [32]. In that sense, CIELAB can be considered a color appearance model, although the adaptation transform, which normalizes the stimulus tristimulus values by those of the reference white, is clearly less accurate than transformations that follow known visual physiology more closely [33]. The CIE does not recommend that CIELAB be used when the illuminant is "too different from that of average daylight" [34]. To investigate how that inaccuracy affects the estimate of the number of discernible colors, we embedded some chromatic adaptation models based on the von Kries hypothesis [35] in the CIELAB equations.

The von Kries-type CATs linearly convert tristimulus values to relative cone responses and scale them so that those of the reference white stay constant for both the destination and the source conditions. The long-, medium-, and short-wavelength cone responses, L, M, and S, are transformed from the X, Y, and Z values by using a 3×3 matrix $\mathbf{M}$. The matrix notation can be extended to the calculation of the corresponding colors across two viewing conditions and to explicitly include the transformation from tristimulus values to relative cone responses as follows:

$$\begin{bmatrix} X_d \\ Y_d \\ Z_d \end{bmatrix} = \mathbf{M}^{-1}\begin{bmatrix} L_{w,d}/L_{w,s} & 0 & 0 \\ 0 & M_{w,d}/M_{w,s} & 0 \\ 0 & 0 & S_{w,d}/S_{w,s} \end{bmatrix}\mathbf{M}\begin{bmatrix} X_s \\ Y_s \\ Z_s \end{bmatrix}, \quad (3)$$

where subscripts d and s denote the destination and the source, respectively, and L_w, M_w, and S_w are the long-, medium-, and short-wavelength cone responses, respectively, of the reference white. The normalization in CIELAB can be expressed by letting $\mathbf{M}$ be the 3×3 identity matrix.

We used three different von Kries-type CATs: CAT02, Hunt–Pointer–Estévez (HPE), and the linearized version of

the Bradford CAT (BFD). CAT02 converts CIE tristimulus values to RGB responses with the "sharpened" cone responsivities, which are spectrally distinct and partially negative, whereas the HPE fundamentals more closely represent actual cone responsivities [33]. CAT02 is used for chromatic adaptation in CIECAM02, whereas HPE is used for post-adaptation. BFD is commonly used for the profile connection space (PCS) required for International Color Consortium profiles in color management [36]. The 3×3 matrices for CAT02 ($\mathbf{M}_{\mathrm{CAT02}}$), HPE ($\mathbf{M}_{\mathrm{HPE}}$), and BFD ($\mathbf{M}_{\mathrm{BFD}}$) are described as follows:

$$\mathbf{M}_{\mathrm{CAT02}} = \begin{bmatrix} 0.7328 & 0.4296 & -0.1624 \\ -0.7036 & 1.6975 & 0.0061 \\ 0.0030 & 0.0136 & 0.9834 \end{bmatrix}, \tag{4}$$

$$\mathbf{M}_{\mathrm{HPE}} = \begin{bmatrix} 0.38971 & 0.68898 & -0.07868 \\ -0.22981 & 1.18340 & 0.04641 \\ 0.00000 & 0.00000 & 1.00000 \end{bmatrix}, \tag{5}$$

$$\mathbf{M}_{\mathrm{BFD}} = \begin{bmatrix} 0.8951 & 0.2664 & -0.1614 \\ -0.7502 & 1.7135 & 0.0367 \\ 0.0389 & -0.0685 & 1.0296 \end{bmatrix}. \tag{6}$$

We used CIECAM02 and CAM02-UCS to verify the estimates of Martínez-Verdú *et al.* [20], Morovic [22], and Morovic *et al.* [23]. CIECAM02 is the latest color appearance model recommended by the CIE. In our simulation, we assumed an average surround condition with three parameters ($F = 1$, $c = 0.69$, and $N_c = 1.0$). The adaptation luminance L_A (in $\mathrm{cd/m^2}$), which is often taken to be 20% of the luminance of the reference white, was calculated using the illuminance of the reference white in lux, E_w,

$$L_A = nE_w/\pi, \tag{7}$$

where $n = 0.2$. The source tristimulus values were converted to cone responses L_s, M_s, and S_s using the CAT02 transform matrix. Next, the cone responses were converted to adapted tristimulus responses L_c, M_c, and S_c representing the corresponding colors under an implied equal-energy illuminant reference condition:

$$L_c = (100D/L_{s,w} + 1 - D)L_s, \tag{8}$$

$$M_c = (100D/M_{s,w} + 1 - D)M_s, \tag{9}$$

$$S_c = (100D/S_{s,w} + 1 - D)S_s, \tag{10}$$

where D is a parameter characterizing the degree of adaptation. D was computed as a function of the adaptation luminance L_A and surround F:

$$D = F(1 - (1/3.6)e^{-(L_A+42)/92}). \tag{11}$$

Theoretically, D ranges from 0 for no adaptation to 1 for complete adaptation. As a practical limitation, it rarely goes below 0.6. After adaptation, the cone responses were converted to the HPE responses L', M', and S'. The post-adaptation cone responses L'_a, M'_a, and S'_a were modified to avoid calculating the power of negative numbers:

$$L'_a = \frac{L'/|L'| \cdot 400(F_L|L'|/100)^{0.42}}{27.13 + L'/|L'| \cdot 400(F_L|L'|/100)^{0.42}} + 0.1, \tag{12}$$

where F_L is the luminance-level adaptation factor:

$$F_L = 0.2k^4(5L_A) + 0.1(1 - k^4)^2(5L_A)^{1/3}, \tag{13}$$

$$k = 1/(5L_A + 1). \tag{14}$$

M'_a and S'_a are described by replacing L' in Eq. (12) with M' and S', respectively. These modifications were necessary because the bandwidth of the spectral reflectance $R(l)$ of optimal colors can become extremely narrow during optimization, producing negative responses. The lightness J, chroma C, colorfulness M, and hue h were then computed. The ratio of colorfulness M to chroma C was calculated as

$$M = C \cdot F_L^{1/4}. \tag{15}$$

The Cartesian coordinates for the chroma (a_C, b_C) and colorfulness (a_M, b_M) are $(C\cos(h), C\sin(h))$ and $(M\cos(h), M\sin(h))$, respectively.

CIECAM02 does not necessarily assume a color space that is perceptually uniform in terms of color differences. To allow a uniform color space to be used, Luo *et al.* [25] built a CIECAM02-based uniform color space (CAM02-UCS) by making the following modifications to the CIECAM02 lightness and colorfulness:

$$J' = 1.7J/(1 + 0.007J), \tag{16}$$

$$M' = (1/0.0028)\ln(1 + 0.0028M). \tag{17}$$

The Cartesian coordinates (a', b') are $(M'\cos(h), M'\sin(h))$.

C. Estimation of the Number of Discernible Colors

The estimate of the number of discernible colors in a color solid depends on the counting method (square-packing, ellipse-packing, or convex-hull) used. The square-packing and convex-hull methods assume a unit cube to be one discernible color in a Euclidean color space. Sphere/ellipse packing is reported to underestimate the number of discernible colors [37].

In the square-packing method, the number of unit squares packed in each locus embodying a solid is counted [18,20]. Estimates based on this method fluctuate, however, depending on the sampling sites. Figure 5 illustrates the square-packing method. The solid line is a true locus; the dotted and solid squares are squares with different sampling sites. The number of squares in the locus differs depending on the sampling sites (13 dotted squares and 19 solid squares). Rather, the area can be used to approximate the number of discernible colors in the locus without such ambiguities if each locus contains many color difference unit squares. The convex-hull method is another popular method of estimating the area enclosed by a locus or the volume of a solid. The

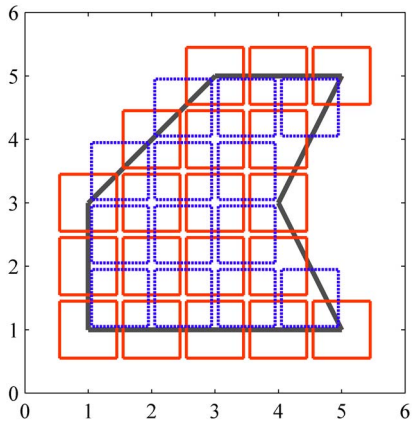

Fig. 5. (Color online) Diagram of square-packing method. The solid line is a true locus; the dotted and solid squares are squares with different sampling sites.

method fails, however, if the locus or solid has concavities. For example, the convex-hull area of the locus shown in Fig. 5 is overestimated to be 14.

As in the square-packing and convex-hull methods, we assumed a unit cube to be one discernible color in a Euclidean color space because this was suitable for verifying some previous estimates and finding the source of the inconsistent figures. Assuming that the volume of a large color solid approximates the number of discernible colors within the solid, we calculated the volume of optimal-color solids in the CIELAB (L^*, a^*, b^*), CIECAM02 $[(J, a_C, b_C)$ and $(J, a_M, b_M)]$, and CAM02-UCS (J', a', b') color spaces. First, 100 optimal-color loci were obtained at lightness values from 0.5 to 99.5 at intervals of 1 for each viewing condition and color space. Each locus consisted of 3001 optimal colors with central wavelengths between 400 and 700 nm at 0.1 nm intervals. The approximate volume of each color solid was obtained by summing the areas of the loci. The area of each convex or concave locus specified by the N vertices of (a_k, b_k), $k = 1, 2, \ldots, N$, was easily calculated by the shoelace algorithm, which can compute the area of a simple polygon whose vertices are described by ordered pairs in the plane as $|\Sigma_{k=1}^{N}(a_k b_{k+1} - a_{k+1} b_k)|/2$, where $a_{N+1} = a_1$ and $b_{N+1} = b_1$.

To verify the estimate of Wen [19], we computed the number of CIE94 color differences within the optimal-color solid in the CIELAB color space. Wen sliced an optimal-color solid at each lightness unit and divided each slice into concentric rings, like onion rings. Each ring, one CIE94 unit chroma thick, was chopped into noncubic dice at intervals of the CIE94 unit hue. Then, he counted the dice to obtain the number of CIE94 color differences or the number of discernible colors within the solid. Some rings were fragmentary because of the distorted shape of the solid, and the estimate depended on the sampling sites.

We took an analytical approach. The color difference ΔE_{94}^* is represented as

$$\Delta E_{94}^* = \sqrt{\left(\frac{\Delta L^*}{k_L S_L}\right)^2 + \left(\frac{\Delta C_{ab}^*}{k_C S_C}\right)^2 + \left(\frac{\Delta H_{ab}^*}{k_H S_H}\right)^2}, \tag{18}$$

$$\Delta H_{ab}^* = \sqrt{\Delta E_{ab}^{*\,2} - \Delta L^{*2} - \Delta C_{ab}^{*\,2}}, \tag{19}$$

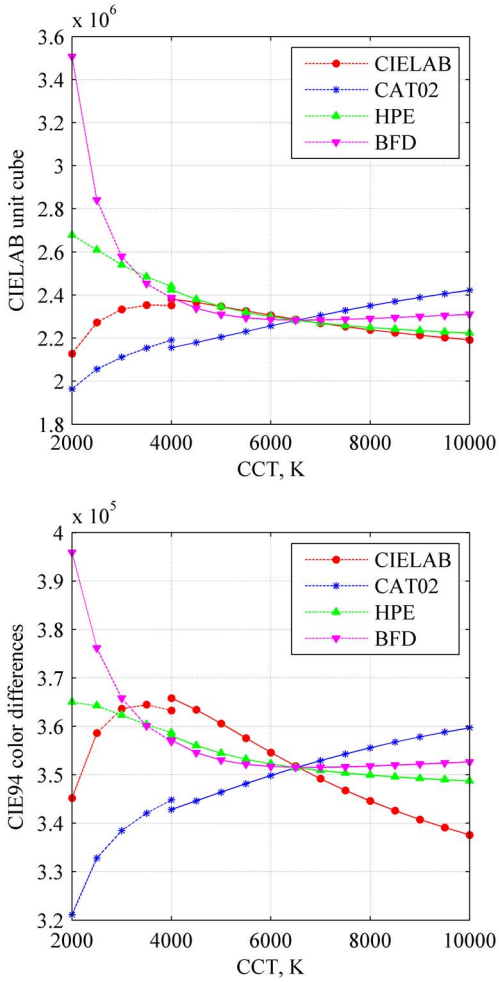

Fig. 6. (Color online) Volume of optimal color solids in the CIELAB unit cube (top) and the number of CIE94 color differences (bottom) calculated with and without the von Kries-type CATs (CAT02, HPE, and BFD) embedded in front of CIELAB as a function of the CCT of the light sources (dotted curves, blackbody radiator; solid curves, daylight illuminant).

$$S_C = 1 + k_1 \sqrt{C_{ab}^*(C_{ab}^* + \Delta C_{ab}^*)}, \tag{20}$$

$$S_H = 1 + k_2 \sqrt{C_{ab}^*(C_{ab}^* + \Delta C_{ab}^*)}, \tag{21}$$

where $S_L = 1$, $k_1 = 0.045$, and $k_2 = 0.015$. We set the parametric factors equal to unity: $k_L = k_C = k_H = 1$. For simplicity, we denote $\Delta C_{94}^* = \Delta C_{ab}^*/S_C$ and $\Delta H_{94}^* = \Delta H_{ab}^*/S_H$; Eq. (18) is then expressed as

$$\Delta E_{94}^* = \sqrt{\Delta L^{*2} + \Delta C_{94}^{*\,2} + \Delta H_{94}^{*\,2}}. \tag{22}$$

If the two colors have a constant lightness value and hue,

$$\Delta C_{94}^* = \frac{\Delta C_{ab}^*}{1 + k_1 \sqrt{(C_{ab}^* + \Delta C_{ab}^*) C_{ab}^*}}. \tag{23}$$

By taking the limit of Eq. (23), a differential equation for the chroma is derived as follows:

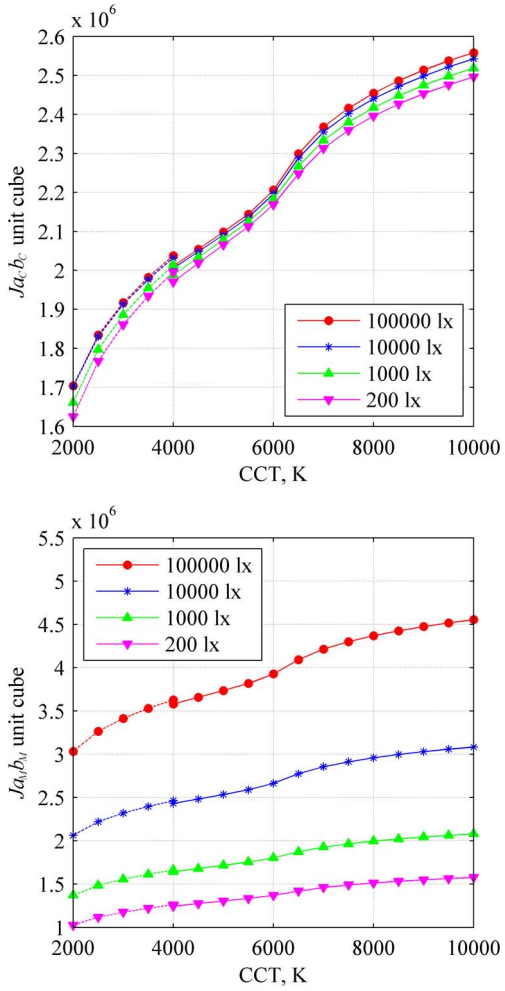

Fig. 7. (Color online) Volume of optimal color solids in the CIECAM02 lightness–chroma (top) and lightness–colorfulness (bottom) spaces as a function of the CCT of the light sources with the illuminance of the reference white of 200, 1000, 10,000, and 100,000 lx (dotted curves, blackbody radiator; solid curves, daylight illuminant).

$$\frac{dC^*_{94}}{dC^*_{ab}} = \lim_{\Delta C^*_{ab}\to 0}\frac{\Delta C^*_{94}}{\Delta C^*_{ab}} = \frac{1}{1+k_1C^*_{ab}}. \tag{24}$$

Next, consider that the two colors have a constant chroma of $C^*_{ab}/\cos(\Delta h_{ab}/2)$, at the midpoint of which is C^*_{ab}, and a constant lightness value. When $|\Delta h_{ab}| \ll 1$,

$$\Delta H^*_{ab} = 2C^*_{ab}\tan(\Delta h_{ab}/2) \approx C^*_{ab}\Delta h_{ab}. \tag{25}$$

Then ΔH_{94} is approximated as

$$\Delta H^*_{94} \approx \frac{C^*_{ab}\Delta h_{ab}}{1+k_2C^*_{ab}}. \tag{26}$$

Consider an isosceles triangle whose base is ΔH^*_{94} and height is C^*_{ab}; when its apex is positioned at the achromatic point ($a^* = b^* = 0$), the number of CIE94 color differences ΔA^*_{94} within the triangle is approximately

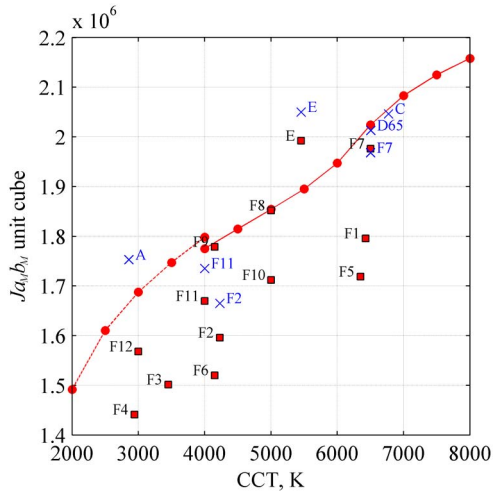

Fig. 8. (Color online) Volume of optimal color solids in the CIECAM02 lightness–colorfulness space as a function of the CCT of the light sources with the illuminance of the reference white of 1571 lx (dotted curve, blackbody radiator; solid curve, daylight illuminant; squares, illuminant series F and illuminant E; crosses, estimate of Martínez-Verdú *et al.* [20]).

$$\Delta A^*_{94} = \int_0^{C^*_{ab}} \Delta H_{94}\mathrm{d}C^*_{94} \approx \int_0^{C^*_{ab}} \frac{C^*_{ab}\Delta h_{ab}}{1+k_2C^*_{ab}}\frac{\mathrm{d}C^*_{ab}}{1+k_1C^*_{ab}}$$
$$= \Delta h_{ab}\cdot\frac{k_1\ln(k_2C^*_{ab}+1) - k_2\ln(k_1C^*_{ab}+1)}{k_1k_2(k_1-k_2)}. \tag{27}$$

Given that the nth optimal color of N points enclosing a two-dimensional area has a hue difference $\Delta h_{ab}(n)$ and chroma $C^*_{ab}(n)$, $\Delta h_{ab}(n) = (h_{ab}(n-1) - h_{ab}(n+1))/2$. Note that $\Delta h_{ab}(n)$ may be negative. The number of CIE94 color differences in the area enclosed by a locus consisting of N optimal colors is calculated as $\Sigma_{n=1}^{N}\Delta A^*_{94}(n)$, where $h_{ab}(0) = h_{ab}(N)$ and $h_{ab}(N+1) = h_{ab}(1)$. The total number of CIE94 color differences within an optimal-color solid is calculated by summing the number of CIE94 color differences within 100 loci obtained in the CIELAB color space.

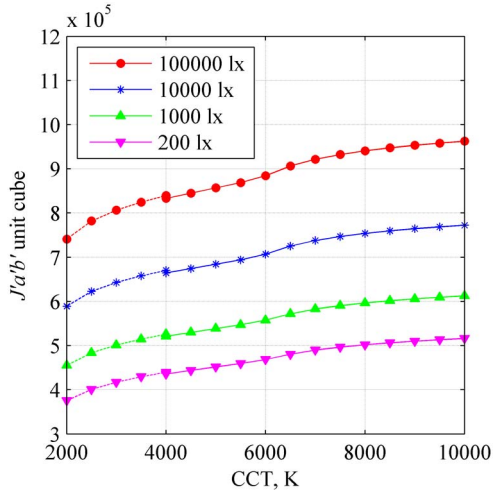

Fig. 9. (Color online) Volume of optimal color solids in the CAM02-UCS space as a function of the CCT of the light sources with the illuminance of the reference white of 200, 1000, 10,000, and 100,000 lx (dotted curves, blackbody radiator; solid curves, daylight illuminant).

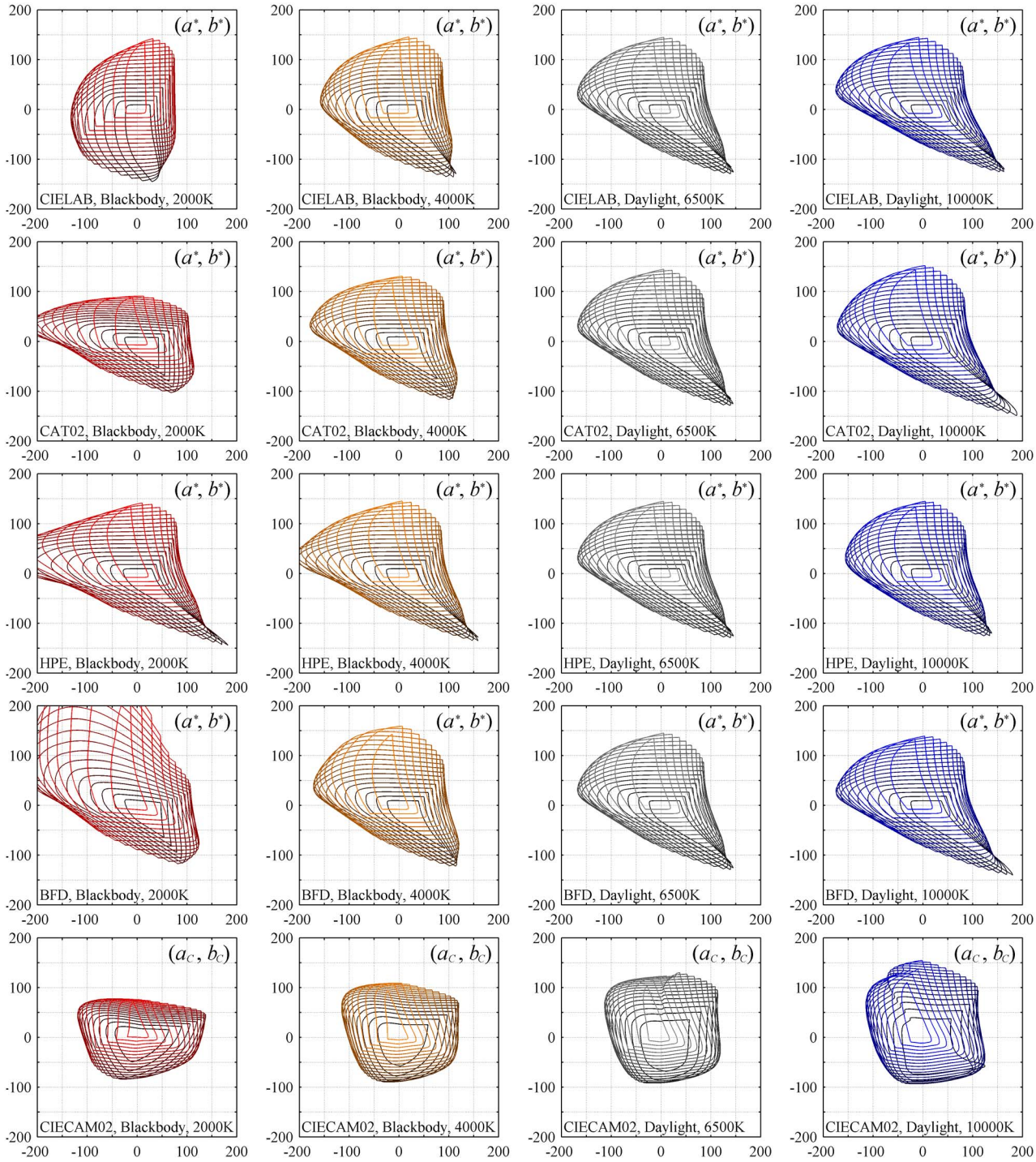

Fig. 10. (Color online) Top view of the loci of optimal color solids in the CIELAB color space computed with and without the von Kries-type CATs (CAT02, HPE, and BFD) and in the CIECAM02 lightness–chroma space (J, a_C, b_C) under blackbody radiators at 2000 and 4000 K and daylight illuminants at 6500 and 10,000 K (1000 lx) for lightness values from 5.5 to 95.5 at intervals of 5 (instead of intervals of 1 to avoid printing too many lines).

3. RESULTS

A. CIELAB-Based Analysis

Figure 6 shows the volume of optimal-color solids in the CIELAB color space (top) and the number of CIE94 color differences (bottom) as a function of the CCT of the light sources, which consisted of blackbody radiators (2000–4000 K) and daylight illuminants (4000–10,000 K). The volumes were calculated with and without the von Kries-type CATs (CAT02, HPE, and BFD) embedded in front of CIELAB. The results clearly show that the number of discernible colors and the variation with the CCT of the adaptation light source depend on the color model used. The breaks in the curves at 4000 K are due to the switch from the spectral power distribution of the blackbody radiator to that of the daylight illuminant. The estimated number of colors at a CCT of 6500 K is 2,286,919 in the CIELAB unit cube, which is close to Pointer

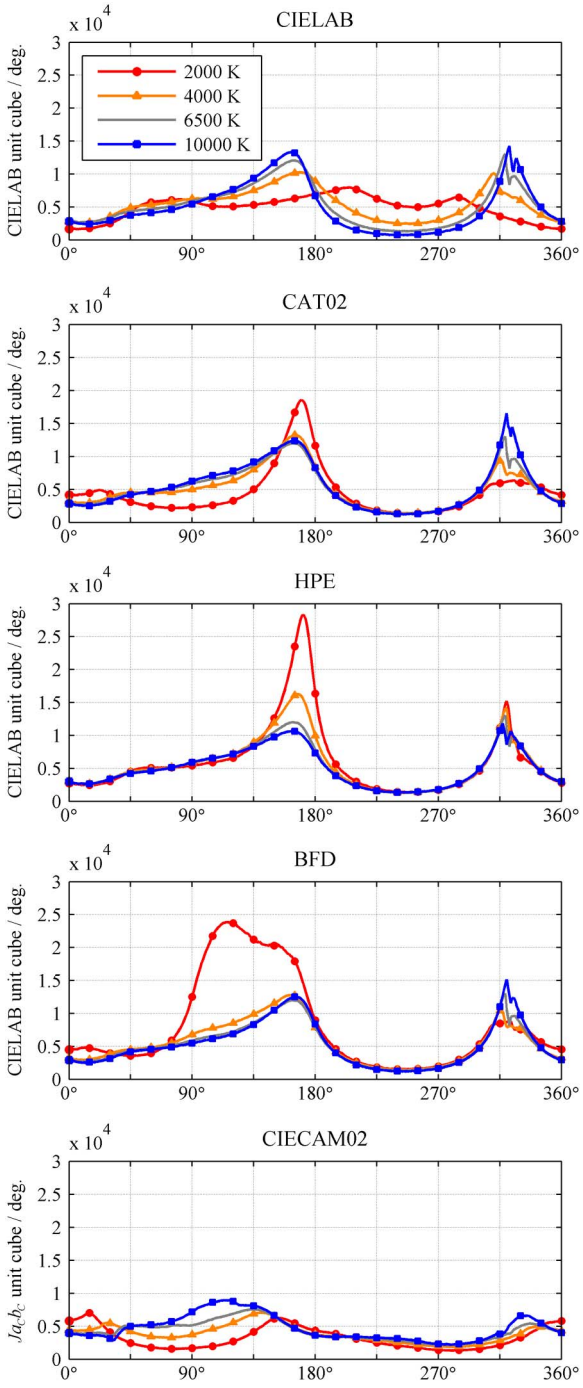

Fig. 11. (Color online) Hue angular volume of optimal color solids in the CIELAB color space computed with and without the von Kries-type CATs (CAT02, HPE, and BFD) and in the CIECAM02 lightness–chroma space (J, a_C, b_C) under blackbody radiators at 2000 and 4000 K and daylight illuminants at 6500 and 10,000 K (1000 lx).

and Attridge's [18] estimate of 2.28 million, and the number of CIE94 color differences is 351,791, which is close to Wen's [19] estimate of 352,263. These estimates are very sensitive to the limen chosen [38]. Considering that one JND corresponds to half of the CIE94 unit, the estimate for the number of discernible colors should be larger than the number of CIE94 color differences by a factor of eight. At 6500 K, the volume is estimated to be 2,110,746, which is again close to Pointer and Attridge's estimate.

B. CIECAM02-Based Analysis

Figure 7 shows the volume of optimal-color solids in the CIECAM02 (J, a_C, b_C) and (J, a_M, b_M) spaces as a function of the CCT for E_w values of 200, 1000, 10,000, and 100,000 lx. Morovic *et al.*'s [23] estimate of 3.8 million Ja_Cb_C cubes under illuminant D50 with an E_w of about 1000 lx is considerably larger than our estimate of 2,078,589, although our result is slightly larger than Morovic's previous estimate of 1.9 million in his book [22], despite his use of the convex-hull method. The former discrepancy is due to miscalculation on their part; the latter is due to the somewhat sparse sampling of optimal colors in his computation [39]. Figure 8 shows the results of Martínez-Verdú *et al.* [20] and our estimate for an E_w value of 1571 lux ($L_A = 100$). These results are similar, although their highest number under illuminant E does not match ours. Figure 9 shows the volume of optimal-color solids in the CAM02-UCS (J', a', b') space as a function of the CCT for E_w values of 200, 1000, 10,000, and 100,000 lx. The volume increases as the CCT and illuminance of the reference white increase, which is the same trend as in Fig. 7 (bottom), although the estimate is relatively small.

4. DISCUSSION

The tendencies in the estimations are determined mainly by the CAT. As shown in Fig. 6, the volume estimated using CIELAB (without the von Kries-type CATs) peaks at around 4000 K. The estimates made using CAT02 increase as the CCT increases, whereas those made using HPE and BFD decrease. The CIECAM02 estimates (Fig. 7) increase as the CCT increases, which is reasonable because the CAT02 chromatic adaptation transform is the main component of CIECAM02. On the whole, the estimates of standard illuminants shown in Fig. 8 also increase with the CCT, despite the dependence on the illuminant spectra. The CAM02-UCS estimates also increase with the CCT for the same reason as for the CIECAM02 estimates.

Figure 10 shows the top view of the loci of optimal-color solids in the CIELAB color space computed with and without the von Kries-type CATs (CAT02, HPE, and BFD) and in the CIECAM02 (J, a_C, b_C) color space under blackbody radiators at 2000 K and 4000 K and daylight illuminants at 6500 K and 10,000 K (1000 lx). Figure 11 shows the corresponding hue angular volume. CAT02 and CIECAM02 exhibit essentially the same trends in the hue angular volume: the yellow component increases as the CCT increases, although the shapes of the loci differ depending on the chromatic adaptation model. The matrix coefficients of CAT02 in Eq. (4) and BFD in Eq. (6) are relatively close to each other, whereas the shapes of the loci differ. These results indicate that a slight difference in the coefficients of the CAT matrices produces different trends in volume estimation.

As shown in Fig. 7, the estimates in the CIECAM02 lightness–chroma space (J, a_C, b_C) and lightness–colorfulness space (J, a_M, b_M) increase as the CCT increases. However, the former is approximately independent of the adaptation luminance level, whereas the latter increases with the illuminance of the reference white E_w. This is reasonable from the relationship between chroma and colorfulness described in Eq. (15). When $L_A \gg 1$, the fourth power of k in Eq. (14) is approximated as zero, and Eq. (13) is then reduced to $F_L \approx 0.1(5L_A)^{1/3} = 0.1(E_w/\pi)^{1/3}$. Then $M = 0.79C$ for E_w

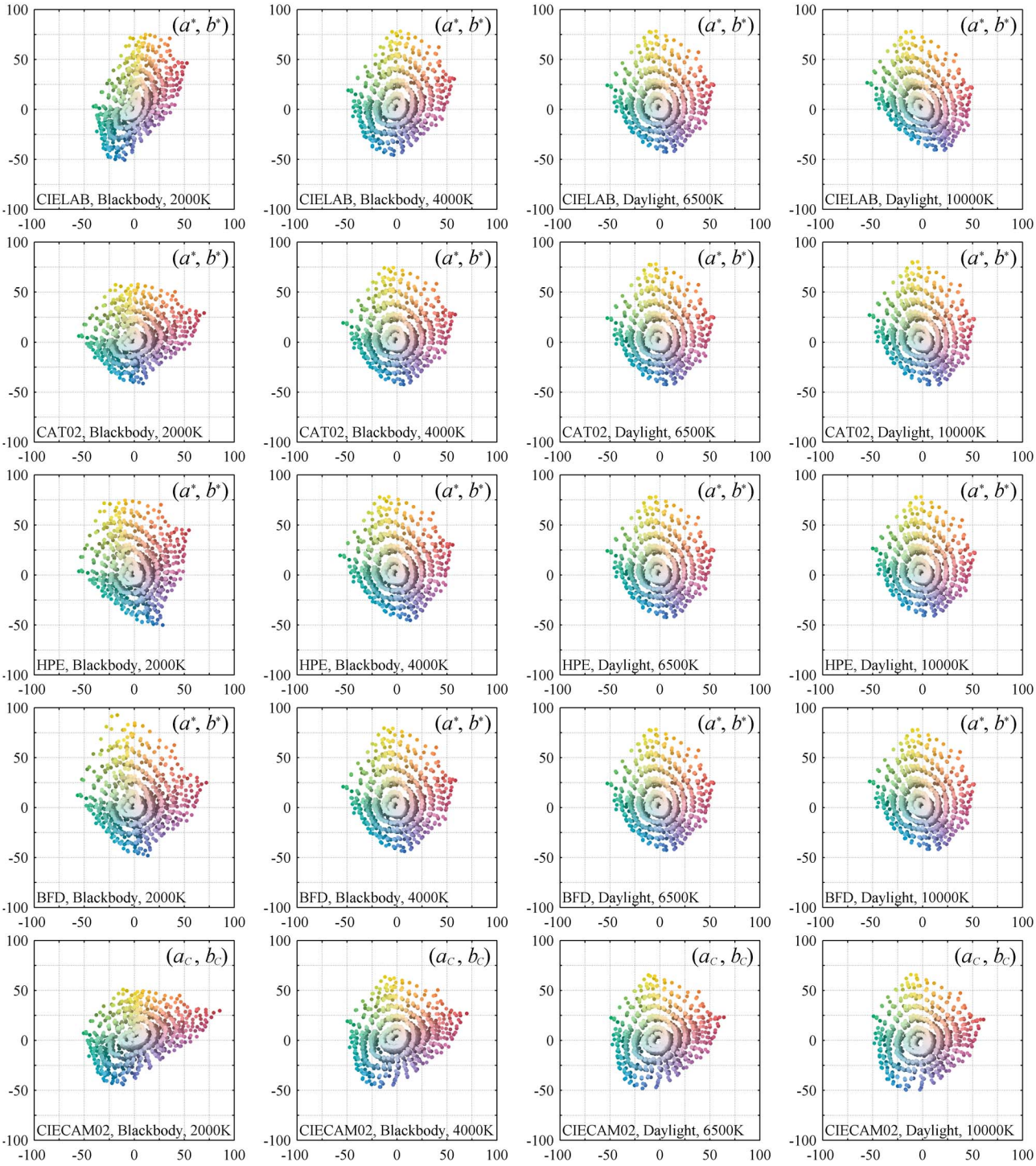

Fig. 12. (Color online) Chromaticity distributions of the Munsell matte colors in the CIELAB color space computed with and without the von Kries-type CATs (CAT02, HPE, and BFD) and in the CIECAM02 lightness–chroma space (J, a_C, b_C) under blackbody radiators at 2000 and 4000 K and daylight illuminants at 6500 and 10,000 K (1000 lx). The marker color represents the Munsell matte colors simulated under illuminant D65.

values of 200 lx, $M = 0.91C$ for 1000 lx, $M = 1.10C$ for 10,000 lx, and $M = 1.33C$ for 100,000 lx. The volume ratios in lightness–colorfulness to lightness–chroma are then roughly 0.63∶1 for 200 lx, 0.83∶1 for 1000 lx, 1.21∶1 for 10,000 lx, and 1.78∶1 for 100,000 lx.

It might be reasonable to use CAM02-UCS rather than CIECAM02 for the estimation because CIECAM02 was originally designed as a color appearance model, not a uniform color space in terms of color differences. The significant dependence of the volume estimation on the illuminance of the reference white is, however, not taken into account. The CIECAM02 lightness–colorfulness space was selected for the base color space of CAM02-UCS because its performance factor measure (PF/3) [40] was slightly better in the lightness–colorfulness space than in the lightness–chroma space. However, the combination of lightness and colorfulness is

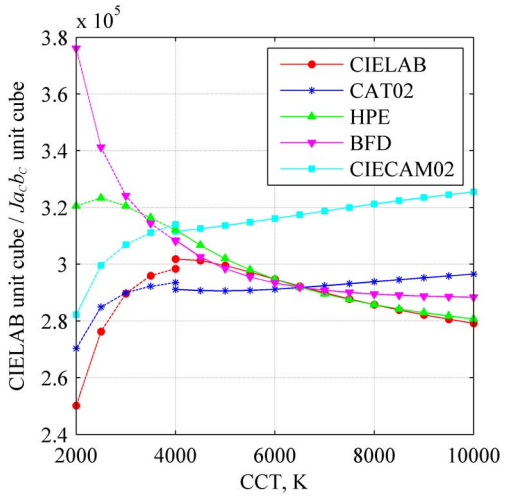

Fig. 13. (Color online) Convex-hull volume of Munsell matte colors in the CIELAB color space calculated with and without the von Kries-type CATs (CAT02, HPE, and BFD) and in the CIECAM02 lightness–chroma space (J, a_C, b_C) as a function of the CCT of the light sources (1000 lx) (dotted curves, blackbody radiator; solid curves, daylight illuminant).

unreasonable because lightness is a relative correlate and colorfulness is an absolute correlate [33]. It seems to be natural in terms of matching the type of scale to use brightness–colorfulness or lightness–chroma, although further study is needed to determine which color space is reasonable for computing the volume of color solids.

Morovic *et al.* [23] noted that any color appearance model fails to estimate the number of discernible colors within an optimal-color solid because the gamut is larger than the psychophysical data it is derived from: for CIECAM02, the LUTCHI data [24] were used. CIELAB has a limitation rooted in its development [41]: it was optimized on the basis of the Munsell system, which is defined only for the CIE 1931 standard observer and illuminant C [42]. We used a dataset [43] consisting of the reflectance spectra of 1269 color chips from the matte edition of the *Munsell Book of Color* as a set of colors with a smaller gamut. Figure 12 shows the chromaticity distributions of the Munsell colors in the CIELAB color space computed with and without the von Kries-type CATs (CAT02, HPE, and BFD) and in the CIECAM02 lightness–chroma space (J, a_C, b_C) under blackbody radiators at 2000 and 4000 K and daylight illuminants at 6500 and 10,000 K (1000 lx). Figure 13 shows the convex-hull volume of the Munsell color solid in the CIELAB unit cube calculated with and without the von Kries-type CATS (CAT02, HPE, and BFD), as well as in the CIECAM02 Ja_Cb_C unit cube, as a function of the CCT of the light sources. The tendencies of increasing and decreasing again depend on the CAT.

If it is assumed that the goal of chromatic adaptation is to maximize color constancy, the adaptation model with the flattest curve is probably the best. If instead it is assumed that

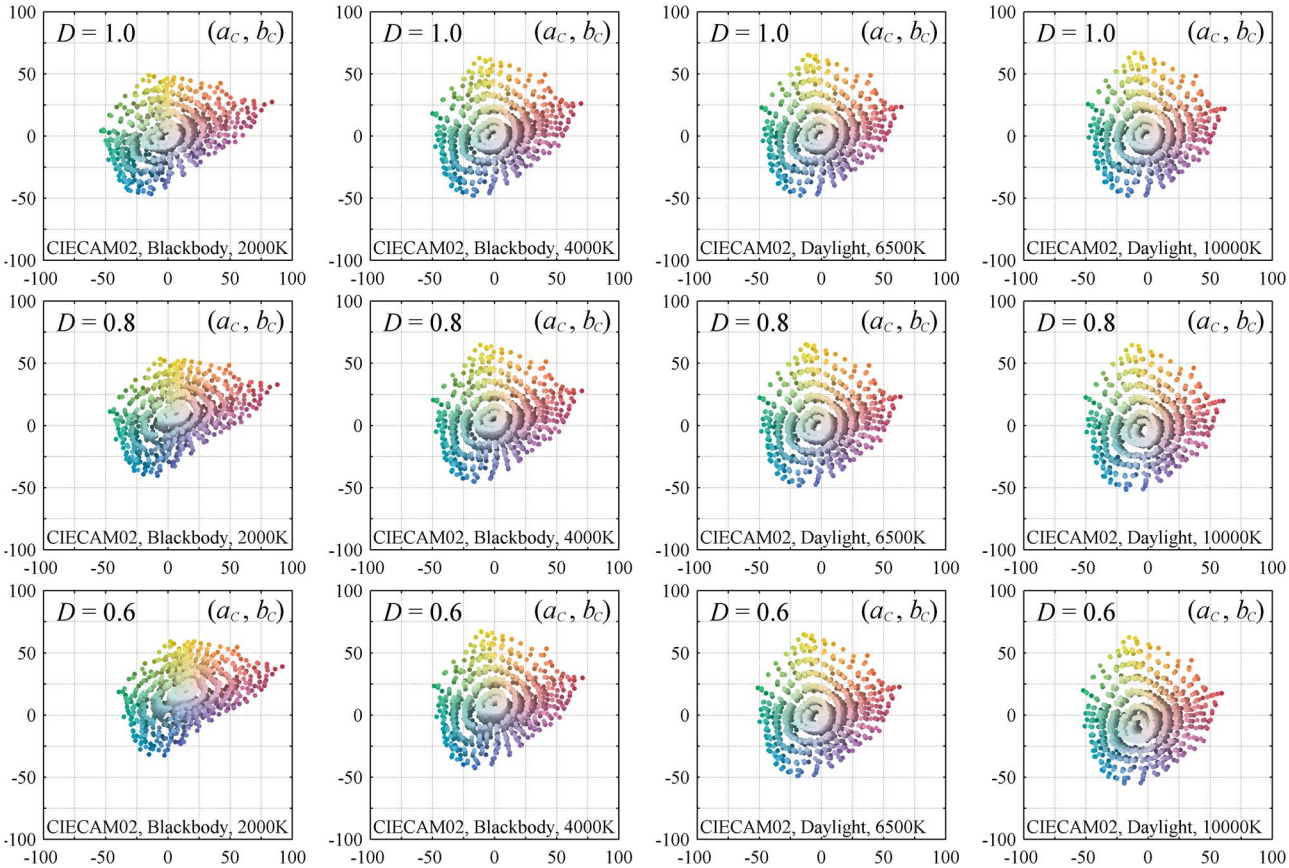

Fig. 14. (Color online) Chromaticity distributions of the Munsell matte colors in the CIECAM02 lightness–chroma space (J, a_C, b_C) under blackbody radiators at 2000 and 4000 K and daylight illuminants at 6500 and 10,000 K (1000 lx) with D factors of 1 (complete adaptation), 0.8, and 0.6 (practical lower limit of incomplete adaptation). The marker color represents the Munsell matte colors simulated under illuminant D65.

chromatic adaptation is about maximizing the number of perceptible colors overall, then maximizing the area might be better (especially at low CCTs and low luminance levels at the beginning and end of the day), and the model with the maximum area might be better. It would be prudent to consider them both to be partial factors. However, it is probably safest to assume that the gamut volume and chromatic adaptation are related only incidentally.

Figure 14 shows the chromaticity distributions of the Munsell colors in the CIECAM02 lightness–chroma space (J, a_C, b_C) under blackbody radiators at 2000 and 4000 K and daylight illuminants at 6500 and 10,000 K (1000 lx) with D factors of 1 (complete adaptation), 0.8, and 0.6 (practical lower limit of incomplete adaptation). Figure 15 shows the volume of the Munsell colors in the CIECAM02 Ja_Cb_C unit cube as a function of the CCT of the light sources. The shapes of the curves representing the volume calculated with CAT02 in Fig. 13 and CIECAM02 ($D = 1$) in Fig. 15 resemble each other. The volume with $D = 0.6$ and $D = 0.8$ in CIECAM02, however, increases unrealistically with the CCT, which indicates a defect in the CAT.

Martínez-Verdú *et al.* [20] suggested the possibility of an alternative color-rendering index based on the number of discernible colors within an optimal-color solid. As shown in Fig. 8, however, their highest number under illuminant E did not match ours because of miscalculation on their part [44]. In either case, the volume estimation depends strongly on the color appearance model used, and the ranking is merely an artifact of CIECAM02. Pinto *et al.* [45,46] conducted subjective experiments to determine the CCT of daylight illumination preferred by observers when appreciating art paintings. They computed the chromatic diversity under daylight illuminants with CCTs of 3600–25,000 K in the CIELAB color space and counted the number of nonempty unit cubes occupied by the corresponding color volume. They found that the distribution of observers' preferences had a maximum at a CCT of about 5100 K and suggested that this preference has a positive correlation with the number of discernible colors. From Figs. 6 and 13, where the volume estimated with CIELAB peaks at around 4000 K, the match between the preference and the number of discernible colors is, however, undeniably coincidental. Masuda and Nascimento [47] investigated illuminant spectra maximizing the theoretical limits of the perceivable object colors. They computed the volume of the optimal-color solid in the CIELAB color space under a large number of metameric illuminants at CCTs of 2222–20,000 K and identified a maximum volume at around 5700 K. They suggested that the estimate of Martínez-Verdú *et al.* that illuminant E (CCT = 5460 K) ranked first in gamut volume, and the positive correlation between a CCT of 5100 K and observers' preferences found by Pinto *et al.* were, along with their findings, possible grounds for the use of the standard illuminant D50 in the printing industry. Quintero *et al.* [48] suggested that colorfulness evaluated on the basis of the volume of optimal-color solids complements the general color-rendering index based on color fidelity. However, as described in Section 2, CIELAB has an intrinsic limitation in the applicable range of its adaptation transform, so comparisons of the volume estimated using CIELAB at different color temperatures are not reliable.

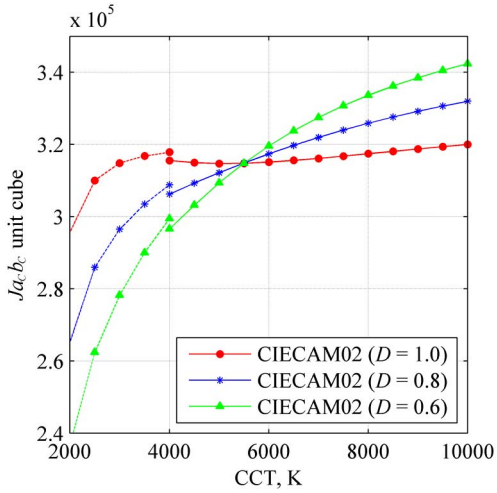

Fig. 15. (Color online) Convex-hull volume of Munsell matte colors in the CIECAM02 lightness–chroma space (J, a_C, b_C) with D factors of 1 (complete adaptation), 0.8, and 0.6 (practical lower limit of incomplete adaptation) as a function of the CCT of the light sources (1000 lx) (dotted curves, blackbody radiator; solid curves, daylight illuminant).

To solve the conundrum, we must find a non-von Kries-type CAT or a completely new color appearance model, but that is well beyond the scope of this paper, or indeed any single paper. There are no documents that clearly and correctly describe the applicable range of the von Kries-type chromatic adaptation in terms of color temperature change for this type of computation. In fact, von Kries had fairly low expectations of his ideas on chromatic adaptation [35], but his work has stood up rather well over the past 100 years. Although our research shows negative results, we believe it is a significant step in the advancement of color science.

5. CONCLUSIONS

We estimated the number of discernible colors over a wide range of color temperatures and illuminance levels using several color models and fast, accurate methods and verified the previous estimates; some estimates are almost the same as ours, and the others are miscalculations on the part of their authors. Our comprehensive simulation revealed that the estimates depend strongly on the color model used. The variations in the volume as a function of the color temperature were determined mainly by the CAT, and slight differences in the coefficients of the CAT matrices caused different trends in the estimation. The applicable range of the von Kries-type chromatic adaptation is unknown in terms of the color temperature change for this type of computation. In particular, the D factor or degree of adaptation incorporated in the CAT matrices has an unnatural effect on the estimate. In addition, the choice between the absolute correlate and the relative correlate significantly affects the dependence of the volume estimation on the illuminance level. As far as the ranking of the number of discernible colors is concerned, further research is required to compare the estimates at different color temperatures and illuminance levels, even if the gamut is small. Thus, the number of discernible object colors remains a conundrum.

APPENDIX A: MATLAB CODE FOR COMPUTING OPTIMAL COLORS WITH A COLOR APPEARANCE MODEL

```
function Lab = optimalcolor_locus(Lc, cmf, S)
% Lc: constant lightness value
% cmf: color-matching functions (N × 3)
% S: illuminant spectrum (N × 1)
T = cmf. * repmat(S(:), [1 3]);
T = T./sum(T(:, 2)) * 100;
XYZws = sum(T);
N = length(T);
T = repmat(T, [3 1]); % concatenation
tol = optimset('MaxIter', 'Inf', 'TolFun', 1e - 10);
for n = 1:N
  fval = inf;
  while fval > 1e - 7||h > N/2||h < 0
    [h fval] = fminsearch(@(x)…
    abs(Lc-optc(T, n + N, x, XYZws)), N/2 * rand, tol);
  end
  [~, Lab(n, :)] = optc(T, n + N, h, XYZws);
end

function [L Lab] = optc(T, n, h, XYZws)
b = n - floor(h): n + floor(h); % body
m = h - floor(h);               % margin
if ~isempty(b)
  Lab = (T(b(1) - 1, :) * m + T(b(1), :) * (2 - m)) * m/2…
      +(T(b(end) + 1, :) * m + T(b(end), :) * (2 - m)) * m/2…
      +sum(T(b, :), 1) - T(b(1), :)/2 - T(b(end), :)/2;
  Lab = your_color_appearance_model(Lab, XYZws);
  L = Lab(1);
else
  L = inf;
end
```

REFERENCES

1. J. Morovic, P. L. Sun, and P. Morovic, "The gamuts of input and output colour imaging media," Proc. SPIE **4300**, 114–125 (2001).
2. R. G. Kuehni, *Color Space and its Divisions: Color Order from Antiquity to the Present* (Wiley, 2003), pp. 202–203.
3. E. B. Titchener, *Outline of Psychology* (Macmillan, 1896), p. 48.
4. E. B. Titchener, *Outline of Psychology: New Edition with Additions* (Macmillan, 1899), p. 55.
5. E. G. Boring, H. S. Langfeld, and H. P. Weld, *Introduction to Psychology* (Wiley, 1939), p. 517.
6. D. B. Judd and K. L. Kelly, "Method of designating colors," J. Res. Nat. Bur. Stand. **23**, 355–366 (1939).
7. D. B. Judd and G. Wyszecki, *Color in Business, Science, and Industry*, 3rd ed. (Wiley, 1975).
8. R. M. Halsey and A. Chapanis, "On the number of absolutely identifiable spectral hues," J. Opt. Soc. Am. **41**, 1057–1058 (1951).
9. A. Hård and L. Sivik, "NCS–natural color system: a Swedish standard for color notation," Color Res. Appl. **6**, 129–138 (1981).
10. W. Ostwald, "Neue Forschungen zur Farbenlehre," Phys. Z. **17**, 322–332 (1916).
11. E. Schrödinger, "Theorie der Pigmente von größter Leuchtkraft," Ann. Phys. **367**, 603–622 (1920).
12. R. Luther, "Aus dem Gebiete der Farbreiz-Metrik," Z. Tech. Phys. **8**, 540–558 (1927).
13. N. D. Nyberg, "Zum Aufbau des Farbkörpers im Raume aller Lichtempfindungen," Z. Phys. **52**, 406–419 (1929).
14. S. Rösch, "Die Kennzeichnung der Farben," Z. Phys. **29**, 83–91 (1928).
15. D. L. MacAdam, "The theory of maximum visual efficiency of colored materials," J. Opt. Soc. Am. **25**, 249–252 (1935).
16. D. L. MacAdam, "Maximum visual efficiency of colored materials," J. Opt. Soc. Am. **25**, 361–367 (1935).
17. D. Nickerson and S. M. Newhall, "A psychological color solid," J. Opt. Soc. Am. **33**, 419–422 (1943).
18. M. R. Pointer and G. G. Attridge, "The number of discernible colours," Color Res. Appl. **23**, 52–54 (1998).
19. S. Wen, "A method for selecting display primaries to match a target color gamut," J. Soc. Inf. Disp. **15**, 1015–1022 (2007).
20. F. Martínez-Verdú, E. Perales, E. Chorro, D. de Fez, V. Viqueira, and E. Gilabert, "Computation and visualization of the MacAdam limits for any lightness, hue angle, and light source," J. Opt. Soc. Am. A **24**, 1501–1515 (2007).
21. "A colour appearance model for colour management systems: CIECAM02," CIE 159:2004 (CIE, 2004).
22. J. Morovic, *Color Gamut Mapping*, 1st ed. (Wiley, 2008), p. 161.
23. J. Morovic, V. Cheung, and P. Morovic, "Why we don't know how many colors there are," in *Proceedings of IS&T CGIV 2012: Sixth European Conference on Colour in Graphics, Imaging, and Vision* (Society for Imaging Science and Technology, 2012), pp. 49–53.
24. M. R. Luo, A. A. Clarke, P. A. Rhodes, A. Schappo, S. A. R. Scrivener, and C. J. Tait, "Quantifying colour appearance. Part I. LUTCHI colour appearance data," Color Res. Appl. **16**, 166–180 (1991).
25. M. R. Luo, G. Cui, and C. Li, "Uniform colour spaces based on CIECAM02 colour appearance model," Color Res. Appl. **31**, 320–330 (2006).
26. "Control of damage to museum objects by optical radiation," CIE 157:2004 (CIE, 2004).
27. "Industrial colour-difference evaluation," CIE 116:1995 (CIE, 1995).
28. K. Masaoka, "Fast and accurate model for optimal color computation," Opt. Lett. **35**, 2031–2033 (2010).
29. G. Wyszecki and W. S. Stiles, *Color Science: Concepts and Methods, Quantitative Data and Formulae* (Wiley, 2000).
30. "Recommended practice for tabulating spectral data for use in colour computations," CIE 167:2005 (CIE, 2005).
31. C. Li, M. R. Luo, M. S. Cho, and J. S. Kim, "Linear programming method for computing the gamut of object color solid," J. Opt. Soc. Am. A **27**, 985–991 (2010).
32. M. D. Fairchild, "Testing colour-appearance models: Guidelines for coordinated research," Color Res. Appl. **20**, 262–267 (1995).
33. M. D. Fairchild, *Color Appearance Models*, 2nd ed. (Wiley, 2005).
34. "Colorimetry," CIE 15.3:2004 (CIE, 2004).
35. J. von Kries, *Chromatic Adaptation, Festschrift der Albercht-Ludwig-Universität* (Fribourg, 1902).
36. P. Green, *Color Management: Understanding and Using ICC Profiles*, 1st ed. (Wiley, 2010).
37. E. Perales, F. Martínez-Verdú, V. Viqueira, M. J. Luque, and P. Capilla, "Computing the number of distinguishable colors under several illuminants and light sources," in *Proceedings of IS&T CGIV 2006: Third European Conference on Colour in Graphics, Imaging, and Vision* (Society for Imaging Science and Technology, 2006), pp. 414–419.
38. C. S. McCamy, "On the number of discernible colors," Color Res. Appl. **23**, 337 (1998).
39. J. Morovic, Hewlett-Packard Ltd., 42 Scythe Way, Colchester, CO3 4SJ, UK (personal communication, 2012).
40. C. Li, M. R. Luo, and G. Cui, "Colour-differences evaluation using colour appearance models," in *Proceedings of IS&T/SID CIC11: Eleventh Color Imaging Conference* (Society for Imaging Science and Technology, 2003), pp. 127–131.
41. R. S. Berns, *Billmeyer and Saltzman's Principles of Color Technology*, 3rd ed. (Wiley-Interscience, 2000), pp. 68–69.
42. S. M. Newhall, D. Nickerson, and D. B. Judd, "Final report of the O.S.A. subcommittee on the spacing of the Munsell colors," J. Opt. Soc. Am. **33**, 385–418 (1943).
43. University of Eastern Finland, Spectral Image Database, http://spectral.joensuu.fi/.
44. E. Perales, Department of Optics, Pharmacology and Anatomy, University of Alicante, Carretera de San Vicente del

Raspeig s/n 03690, Alicante, Spain (personal communication, 2012).
45. P. D. Pinto, J. M. Linhares, J. A. Carvalhal, and S. M. Nascimento, "Psychophysical estimation of the best illumination for appreciation of Renaissance paintings," Vis. Neurosci. **23**, 669–674 (2006).
46. P. D. Pinto, J. M. Linhares, and S. M. Nascimento, "Correlated color temperature preferred by observers for illumination of artistic paintings," J. Opt. Soc. Am. A **25**, 623–630 (2008).
47. O. Masuda and S. M. Nascimento, "Lighting spectrum to maximize colorfulness," Opt. Lett. **37**, 407–409 (2012).
48. J. M. Quintero, C. E. Hunt, and J. Carreras, "De-entangling colorfulness and fidelity for a complete statistical description of color quality," Opt. Lett. **37**, 4997–4999 (2012).